

A comparison of mercury-based cuprate superconductors and aluminum-doped zinc oxide

Oscar Martinez

University of California San Diego, La Jolla, CA 92093, USA

(Dated: Spring 2022)

High-temperature superconductivity is a relatively recent discovery and a field rich in features. However, the underlying physics behind high-temperature superconductivity is still not yet known. Relatively similar materials can have different properties due to various reasons. Here, we present a series of experimental values for the magnetic susceptibility, resistivity, lattice, Hall Coefficient, and specific heat capacity of the family of mercury-based cuprates and aluminum-zinc oxide. These experimental values are compared for similarities and differences to describe the inherent difference in properties between a high-temperature copper oxide superconductor and an oxide conductor.

I. INTRODUCTION

Superconductivity is a property of certain materials wherein no loss of energy is experienced when a current passes through a material. Other unique properties of superconductors include the Meissner effect, where superconductors expel magnetic fields applied to them. There are two types of superconductors: type I and type II. This paper will focus on type II superconductors and in particular high-temperature superconductors.

Type superconductors have unique properties that define them. At the critical temperature, a material experiences a phase transition and becomes a superconductor. Once this temperature is reached, their unique properties show themselves. The first and most notable is a lack of resistivity. Typical conductors have little resistivity, regardless of the conditions. Superconductors forego resistivity and thus lose no power when current is sent through them once their temperature reaches a temperature known as the critical temperature. The second property is the expulsion of any applied magnetic fields [1]. This is known as the Meissner Effect. These properties are indicative of superconductors and will be used to demonstrate superconductivity.

Type II superconductors have a unique property which mirrors the critical temperature. According to the Meissner Effect, superconductors will expel a magnetic field applied to it. This will continue until the strength of the magnetic field is high enough that the superconductor cannot expel the field. The point at which this occurs is called the critical field. Type I superconductors experience a phase change from a superconductor to a conductor. However, type II superconductors remain superconductors until a stronger critical field is applied. This is indicated by a phase change when a magnetic field is swept in strength against the superconductor. Such phase changes are indicative of type II superconductors and will be used to demonstrate type II super-

conductivity.

This paper will compare the properties of a family of high-temperature superconductors, mercury-based cuprates, and a non-superconductor, aluminum-doped zinc oxide. The aim is to demonstrate the properties of a superconductor and compare them to a similar non-superconducting material.

II. ANALYSIS OF MBCCO AND AZO

A. Conductivity and Magnetic Susceptibility

Mercury-based cuprates are a family of hole-doped cuprates, where the doping element is mercury. These cuprates have the chemical formula of $HgBa_2Ca_{n-1}Cu_nO_{2n+2}$, where n is the amount of cuprate planes [2] and are on occasion called MBCCO. The naming convention of members of the family of hole-doped cuprates is the name of the doping agent followed by the amount of each non-oxygen atom in each molecule. As such, $HgBa_2CuO_4$ is referred to as Hg-1201, $HgBa_2CaCu_2O_6$ is Hg-1212, and so on. The properties of mercury-based cuprates as superconductors change based on the amount of cuprate planes. These properties include, but are not limited to, maximum T_c under ambient pressure and max T_c under high pressure [2]. The critical temperature at ambient pressure ranges from 95 K at $n=1$ to 133 K at $n=3$. As more cuprate plates are added, the critical temperature of the material decreases. Lastly, the critical temperature at high pressure ranges from 118 K at $n=1$ to 164 K at $n=3$ [3]. Once again, the critical temperature at high pressure decreases when there are more cuprate plates after three.

Experimental evidence demonstrates changes in magnetic susceptibility for MBCCO [4]. One experiment had an MBCCO sample with 2 cuprate layers had alternating-current magnetic susceptibil-

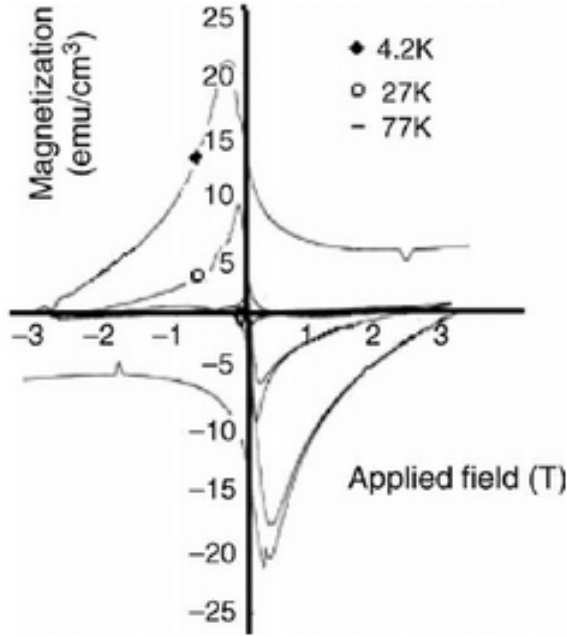


Figure 1: The magnetic susceptibility of MBCCO when an external magnetic field is applied [[5]]

ity measurements taken between 4.2 K and 120 K. At 120 K, MBCCO is paramagnetic. The MBCCO continues to be paramagnetic until the temperature is lowered to 93 K, at which point it experiences a phase transition to become diamagnetic. MBCCO continues to be diamagnetic without experiencing any other phase transitions. Figure 3 shows a plot of the magnetic susceptibility of the experiment. The figure shows a plot of the magnetic susceptibility of MBCCO when there are 3 cuprate plates.

Another group [6] measured the electrical resistivity of an MBCCO sample at varying temperatures ranging from 80 K to 130 K. There is a linear decrease of the resistivity as the temperature decreases until the resistance sharply drops to 0 at 98 K. A visualization of the experimental resistivity values as a function of temperature is shown in figure 2.

The magnetic susceptibility of MBCCO at the critical temperature reveals a phase transition towards diamagnetism. The resistivity also drops towards zero at the same temperature. These properties reveal the superconducting nature of MBCCO.

Furthermore, the hyperbolic nature of the magnetic susceptibility demonstrates that MBCCO is an unconventional type II superconductor. As stated previously, phase changes over a sweeping magnetic field are indicative of type II superconductors.

Aluminum-doped Zinc Oxide, or AZO, is another conductig oxide. However, it is not a superconduc-

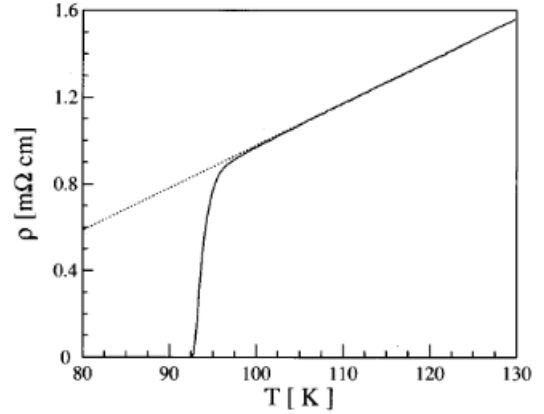


Figure 2: The experimental resistivity values of a sample of Hg-1201 Cuprate as temperature changes. Note the sharp decrease in resistance around 92 K [6]

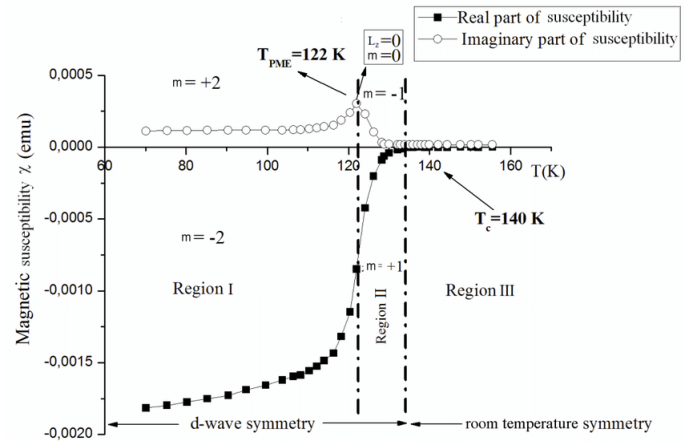


Figure 3: A visualization of the magnetic susceptibility of HG-1223 based cuprate as a function of the temperature [4]

tor. It's resistance is dependent on the quantity of the dopant in the material [7]. The resistivity of the material is the lowest when the ratio between aluminum and zinc is around .8 percent. Figure 4 shows the resistivity as the aluminum doping changes.

The temperature dependence of resistivity in AZO is generally an inverse relationship. The resistivity of AZO drops linearly until around 200 K, after which the rate of decrease of the resistivity relative to the temperature begins to decrease [8]. The exact decrease and the temperature at which the change occurs is dependent on the thickness of the AZO sample. Figure 6 demonstrates the relationship between temperature and resistivity of AZO.

Figures 2 and 4 show how resistivity changes as both the doping and temperature changes. Since the

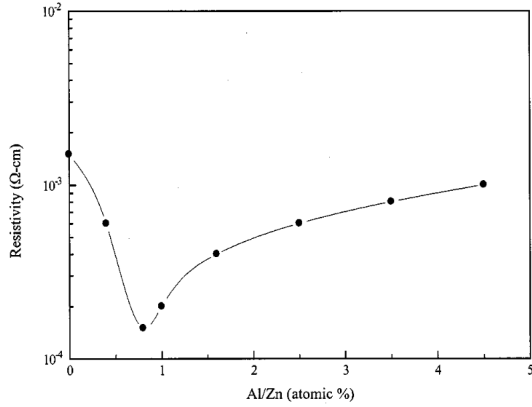


Figure 4: A visualization of the resistivity of AZO as the doping of aluminum changes relative to the zinc in a sample [7]

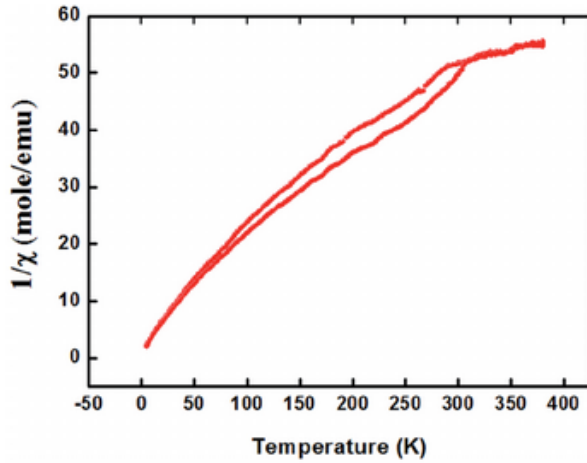


Figure 5: The inverse susceptibility of AZO as a function of temperature [8]

values are not 0 at any point, we can conclude that the resistivity of AZO never becomes 0 and AZO therefore never experiences a phase change and becomes a superconductor. Due to its low resistivity, however, it is a conductor.

The resistivity of AZO and Hg-1201 are both linear up to a point. For Hg-1201, that is the critical temperature. The resistivity of Hg-1201 falls to zero below the critical temperature. However, the rate of decrease for the resistivity of AZO decreases at 200 K. At lower temperatures, the resistivity approaches $1 \times 10^{-4} \Omega \text{cm}$. Below each material's respective transition points, each material exhibits the opposite of the other material: Hg-1201 sharply decreases and AZO flattens when it decreases.

We can also see the difference in magnetic suscep-

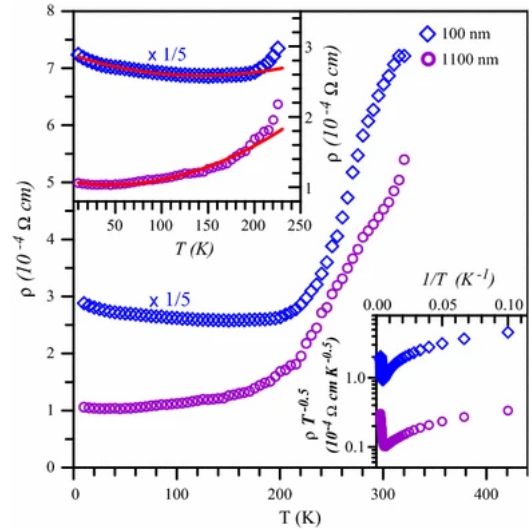


Figure 6: Resistivity of two AZO samples compared to their temperature. The blue sample has a thickness of 100 nm and the purple sample has a thickness of 1100 nm [8]

tibility between Hg-1223 and AZO. The magnetic susceptibility of Hg-1223 is hyperbolic in nature, where it decreases as temperature decreases. By contrast, the susceptibility of AZO increases as temperature decreases. As the temperature increases, the susceptibility of AZO decreases and the rate of change decreases. Since Hg-1223 is hyperbolic, its rate of change as the temperature increases decreases drastically. Thus, AZO and Hg-1223, for the most part, have opposite magnetic susceptibility properties.

B. Lattice

The primitive cell of mercury-based cuprates is separated into discrete layers of Mercury Oxide, copper oxide, barium oxide, and calcium [9]. A visualization of various primitive cells of Hg-1223 is shown in figure 7. At the top end, there is a Mercury Oxide layer. The following layers on each side are Barium Oxide. The remaining layers are a rotation of Copper Oxide and Calcium layers. The amount is dependent on how many Copper Oxide layers there are in the material.

The structure of AZO is based around four Zn_3O bonded around an aluminum atom. The lattice is shown in three dimensions in figure 8 [10].

Here, we can see a difference in the structure of MBCCO and AZO. Individual MBCCO molecules have a linear atomic configuration. By contrast, AZO molecules have a tetrahedral molecule. The

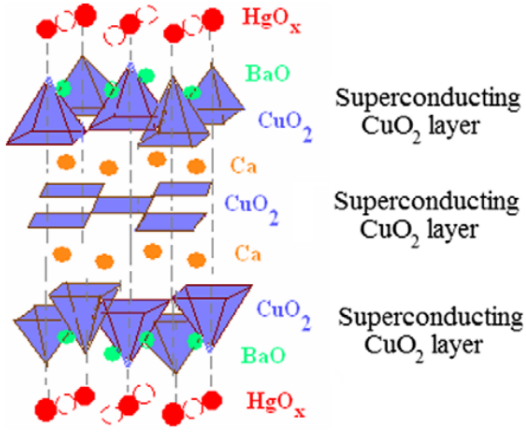


Figure 7: A visualization of Hg-1223 cuprate primitive cells. Here are several primitive cells together [9]

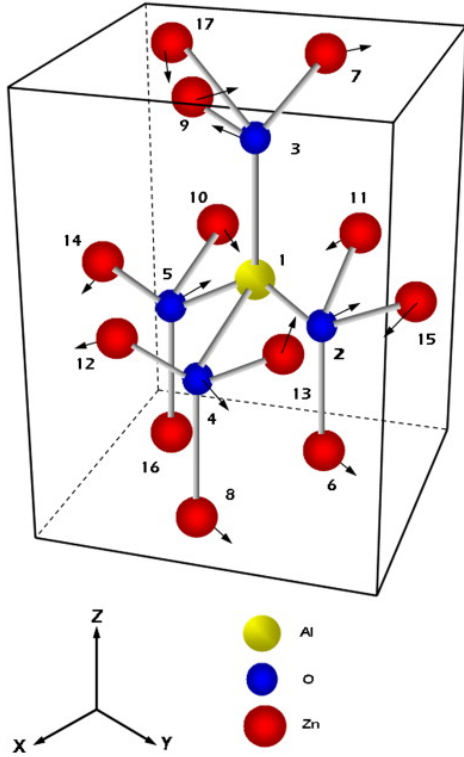


Figure 8: The lattice structure of Aluminum-doped Zinc Oxide in three dimensions [10]

amount of free electrons potentially present in the layers of MBCCO molecules could assist in the superconducting properties of the material. Conversely, there is less potential for free electrons to flow through AZO, as the bond is not linear.

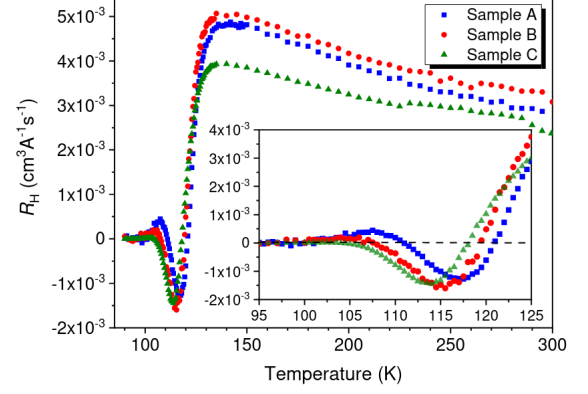


Figure 9: The experimental values of the Hall Coefficient for three prepared samples of Hg-1212. The Hall Coefficient values are measured relative to the temperature of the samples [11]

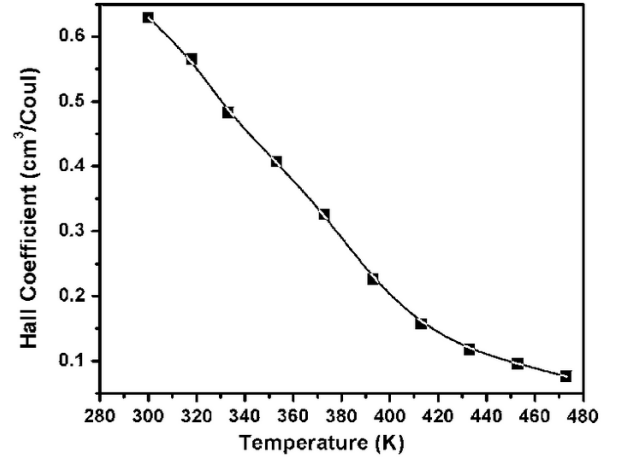


Figure 10: Experimental Hall Coefficient values taken at discrete temperature values [12]

C. Hall Coefficient

Samples of mercury-based cuprates experience a sharp change in their Hall Coefficient values as the temperature reaches the critical temperature [11]. Figure 9 shows how the Hall Coefficient changes as the temperature approaches and surpasses the critical temperature. The Hall Coefficient sharply drops as the temperature approaches the critical temperature from both sides. The Hall Coefficient then sharply increases and decreases at a much lower rate.

By contrast, AZO has a general trend for the Hall Coefficient. As the temperature decreases, the Hall Coefficient increases, which can be seen in Figure 10. Hg-1212 shares the same relationship in that the Hall Effect of both increases as the temperature

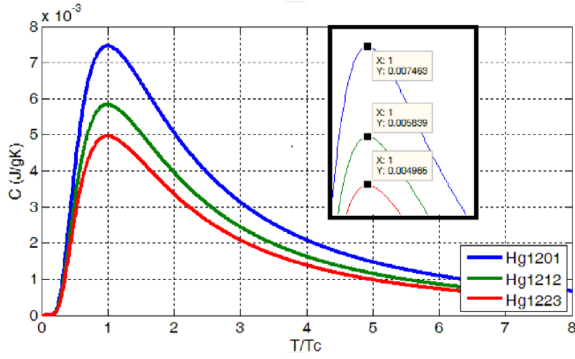


Figure 11: The specific heat capacity for Hg-1201, Hg-1212, and Hg-1223 with respect to the temperature and critical temperature [11]

decreases. This occurs for Hg-1212 until the critical temperature is reached. AZO, however, has no sharp decreases.

D. Specific Heat Capacity

A property of superconductors is that when their temperature is equal to their critical temperature, they experience an increase in their specific heat capacity. This is due to how superconductors experience a phase transition. When a material experiences a phase transition, its specific heat capacity increases [13].

Figure 11 shows the specific heat capacity of various MBCCO compositions when compared to the ratio between the temperature and the critical temperature [11]. When the temperature equals the critical temperature, the specific heat capacity is the highest, regardless of composition. This demonstrates that at the critical temperature, MBCCO experiences a phase transition.

To find the specific heat capacity of AZO, we must first consider the relationship between the specific heat capacity and thermal conductivity. The equation for thermal conductivity is

$$\kappa = C_p v \rho \quad (1)$$

where C_p is the specific heat, v is the thermal diffusivity, and ρ is the density of the sample [15]. We can see that there is a linear relationship between the thermal conductivity and the specific heat of a material.

Now consider figure 12. Since the thermal conductivity is linear, we can safely conclude that AZO, regardless of its structure or method of production, does not experience a phase transition. There is no drastic change in thermal conductivity and therefore

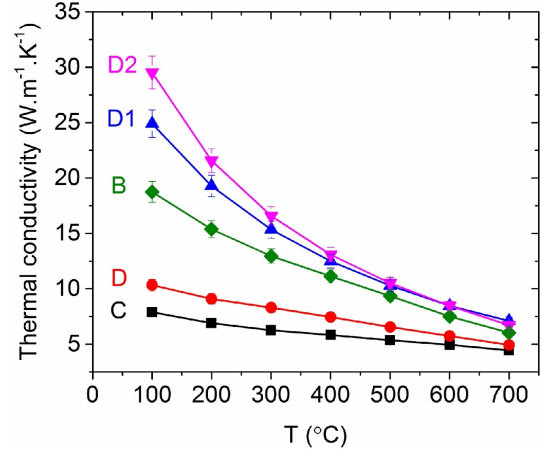


Figure 12: Thermal Conductivity of different samples of AZO. Each sample was prepared differently [14]

no drastic change in the specific heat capacity. This is in contrast to the mercury-based cuprates of figure 10. The thermal conductivity and therefore the specific heat capacity are increasing as the temperature decreases. This mirrors the trend of MBCCO as its temperature decreases towards the critical temperature.

III. CONCLUSION

Discernible similarities and differences are clear and present between mercury-based cuprates and aluminum-doped zinc oxide. These differences can give insight into why mercury-based cuprates are superconductors and aluminum zinc oxide isn't. The key differences in structure may be an underlying factor in why AZO does not experience a phase transition to become a superconductor. The difference in the measured Hall Coefficient trends and the specific heat capacity trends of MBCCO and AZO demonstrate that there is a difference in reaction to temperature. More generally, we see that

IV. ACKNOWLEDGEMENTS

The author would like to thank Dr. Jorge E. Hirsch and the University of California, San Diego for their contributions.

-
- [1] R. Eisberg and R. Resnick, *Quantum Physics of Atoms, Molecules, Solids, Nuclei, and Particles* (John Wiley and Sons, Inc., 1974).
 - [2] C. Chu, L. Deng, and B. Lv, *Physica C: Superconductivity and its Applications* **514**, 290 (2015), superconducting Materials: Conventional, Unconventional and Undetermined.
 - [3] J. Hirsch, M. Maple, and F. Marsiglio, *Physica C: Superconductivity and its Applications* **514**, 1 (2015), superconducting Materials: Conventional, Unconventional and Undetermined.
 - [4] S. N. Putilin, E. V. Antipov, O. Chmaissem, and M. Marezio, *Nature* **362**, 226 (1993).
 - [5] Z. Özdemir, Aslan Çataltepe, and Onbaşlı, *Journal of Physics and Chemistry of Solids* **67**, 453 (2006).
 - [6] R. Masini, R. Eggenhöfner, E. Bellingeri, E. Gianini, and R. Vaccarone, *Applied Physics Letters* **68**, 2282 (1996), <https://doi.org/10.1063/1.115885> .
 - [7] Y. Zhang, W. Wang, R. Tan, Y. Yang, X. Zhang, P. Cui, and W. Song, *International Journal of Applied Ceramic Technology* **9**, 374 (2012), <https://ceramics.onlinelibrary.wiley.com/doi/pdf/10.1111/j.1744-7402.2011.02666.x> .
 - [8] L.-M. Wang, C.-Y. Wang, C.-R. Jheng, S.-J. Wu, C.-K. Sai, Y.-J. Lee, C.-Y. Chiang, and B.-Y. Shew, *Applied Physics A* **122**, 731 (2016).
 - [9] Onbasli, Z. Özdemir, and Aslan Çataltepe, *Chaos Solitons Fractals - CHAOS SOLITON FRACTAL* **42**, 1980 (2009).
 - [10] F. Maldonado and A. Stashans, *Journal of Physics and Chemistry of Solids* **71**, 784 (2010).
 - [11] J. O. Odhiambo (2016).
 - [12] P. Pattanaik, S. Kamilla, D. Das, and D. Mishra, *Journal of Materials Science: Materials in Electronics* **25** (2014), 10.1007/s10854-014-1984-1.
 - [13] D. V. Schroeder, *An Introduction to Thermal Physics* (Oxford University Press, 2011).
 - [14] R. Cebulla, R. Wendt, and K. Ellmer, *Journal of Applied Physics* **83**, 1087 (1998), <https://doi.org/10.1063/1.366798> .
 - [15] K. Cai, E. Müller, C. Drašar, and A. Mrotzek, *Materials Science and Engineering: B* **104**, 45 (2003).